論 文 の 内 容 の 要 旨

論文題目 Syntheses of Ionic Crystals of Polyoxometalate-Organometallic Complex and Sorption Properties
（ポリオキソメタレート－有機金属錯体イオン性結晶の合成とその収着特性）

氏　　名　　アルデスレスバニ （ALDES LESBANI)

（本文）

Introduction

The assembly of molecular or atomic building blocks into ordered solid compounds, which are applicable to selective sorption, separation, and heterogeneous catalysis, has been an attractive research area in material chemistry. Polyoxometalates (POMs) are nano-sized metal-oxide macroanions and have a growing interest as building blocks of ordered solid compounds. However, the combination of POM with a small sized and highly charged cation (e.g., first-row transition metal cation), usually forms a highly soluble solid. The complexation of POMs with appropriate organometallic complexes (macrocations) can create insoluble ionic crystals with specific structures. In this work, porous ionic crystals of polyoxometalate-organometallic complex are synthesized by the control of the shape, size, and charge of the constituent ions and the sorption properties are investigated (Figure 1).

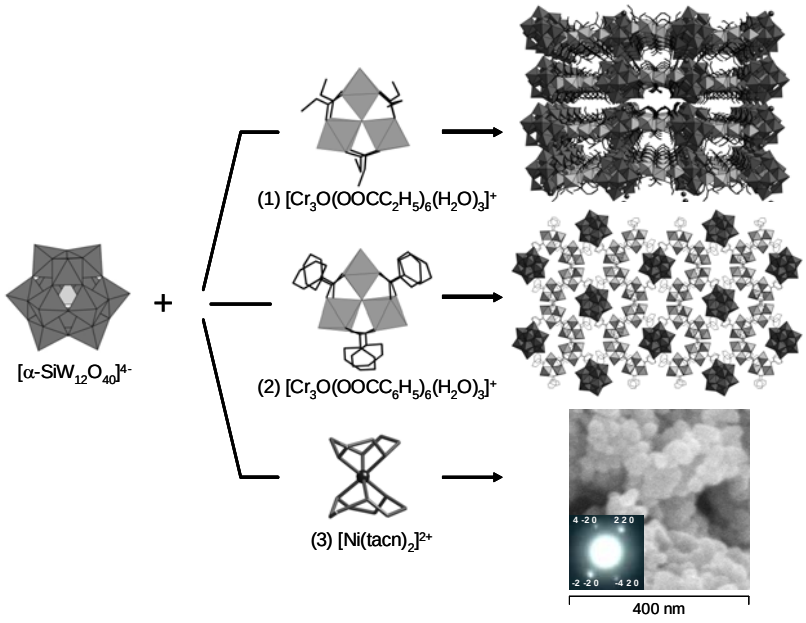

Figure 1. Polyoxometalate-organometallic ionic crystals. (1) Crystal structures of $A_2[Cr_3O(OOCC_2H_5)_6(H_2O)_3]_2[\alpha\text{-}SiW_{12}O_{40}]$ (A = K, Rb, and Cs), (2) $[M_3O(OOCC_6H_5)_6(H_2O)_3]_4[\alpha\text{-}SiW_{12}O_{40}]$ (M = Cr, Fe), and (3) SEM image and electron diffractogram of crystalline nano-particles of $[Ni(tacn)_2]_2[\alpha\text{-}SiW_{12}O_{40}]$ (tacn = 1,4,7-triazacyclononane).

1. Control of structures and sorption properties of ionic crystals of $A_2[Cr_3O(OOCC_2H_5)_6(H_2O)_3]_2[\alpha\text{-}SiW_{12}O_{40}]$ (A = Na, K, Rb, Cs, and TMA)

The complexation of Keggin-type polyoxometalate $[\alpha\text{-}SiW_{12}O_{40}]^{4-}$, macrocation $[Cr_3O(OOCC_2H_5)_6(H_2O)_3]^+$, and monovalent cation A^+ formed ionic crystals of $A_2[Cr_3O(OOCC_2H_5)_6(H_2O)_3]_2[\alpha\text{-}SiW_{12}O_{40}]\bullet n H_2O$ (A = Na [**1a**], K [**2a**], Rb [**3a**], Cs [**4a**], and tetramethylammonium (TMA) [**5a**]). Single crystal and powder X-ray analyses showed that the ionic crystals possess 2D-layers of polyoxometalates and macrocations. Compounds **2a**-**4a** were isostructural, while the layers in **1a** and **5a** stacked in different ways. Among the isostructural guest free phases of **2b**-**4b**, the lengths of the *b*-axes, which are twice the value of the interlayer distance, increased with the increase in the ionic radius of the monovalent cations (**2b** (K^+: 1.52 Å) < **3b** (Rb^+: 1.66 Å) < **4b** (Cs^+: 1.81 Å)), which resided between the layers (Table 1). Compounds **2b**-**4b** possessed hydrophobic and hydrophilic channels, which existed between the layers and through the layers, respectively (Figure 2). The volumes of the hydrophobic channels increased in the order of **2b** < **3b** < **4b** and those of the hydrophilic channels increased in the order of **2b** ≤ **3b** < **4b** (Table 1).

Table 1. Structural Properties of **2b**-**4b**

	2b	**3b**	**4b**
a [Å]	15.85	15.80	15.87
b [Å]	19.25	19.52	1999
c [Å]	30.41	30.50	3047
V [Å^3]	9278	9406	9667
Hydrophilic channel			
Volume [$\mu L^{-1}g$]	19.0 ± 3.0	19.5 ± 3.0	21.0 ± 3.0
Hydrophobic channel			
Volume [$\mu L^{-1}g$]	23.0 ± 3.0	25.0 ± 30	30.0± 3.0
Opening [Å]	2.5 × 5.1	3.4 × 5.1	4.0× 52

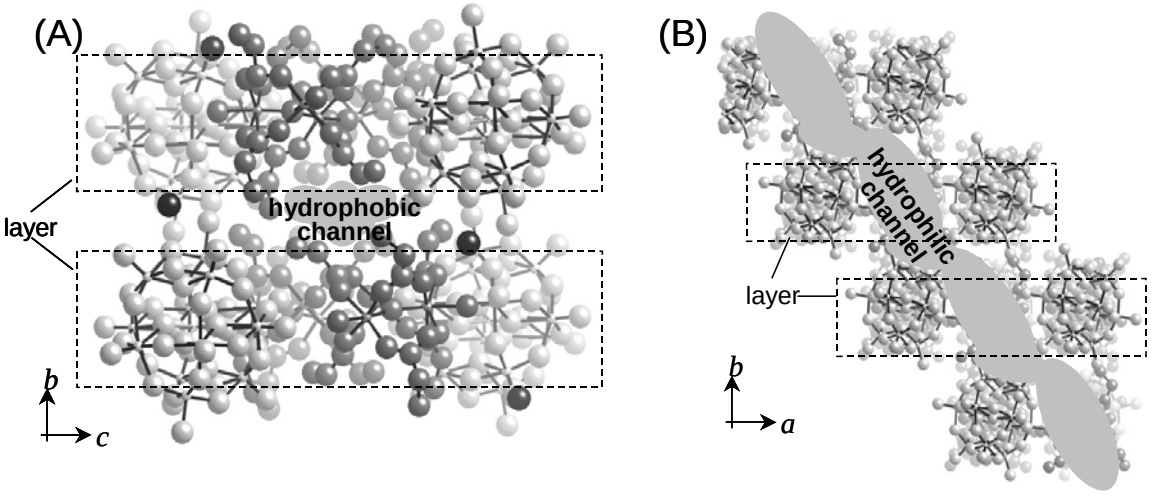

Figure 2. Local structures of $Rb_2[Cr_3O(OOCC_2H_5)_6(H_2O)_3]_2[\alpha\text{-}SiW_{12}O_{40}]$ [**3b**] in the (a) *bc*- and (b) *ab*-plane. Dotted rectangles showed the layers of **3b**. Hydrophilic and hydrophobic channels were indicated by the shadings.

Figure 3 shows the vapor sorption isotherms of **2b**-**4b** at 298 K. The amounts of water sorption increased with the increase in the water vapor pressure and were almost leveled off around P/P_0 = 0.8 (Figure 3A). The amounts of sorption reached up to 19-22 μL g^{-1} at P/P_0 = 0.8, and the values approximately agreed with the volumes of the hydrophilic channels (19-21 μL g^{-1}). The water vapor sorption profiles of **2b**-**4b** were reproduced by a linear driving force model, $M_t = M_e \{1 - \exp(-k_1 t)\}$, suggesting that water is sorbed only in the hydrophilic channel. As for amphiphilic *n*-propanol, the amounts of sorption increased in the order of **2b** ≤ **3b** < **4b** (Figure 3B). The amounts of sorption at P/P_0 > 0.6 exceeded the volumes of the hydrophilic channel, and reached up to 30, 45, and 55 μL g^{-1} for **2b**, **3b**, and **4b**, respectively, of which the values approximately agreed with the sums of the volumes of hydrophilic and hydrophobic volumes. The *n*-propanol sorption profiles were reproduced by the summation of the linear driving force model, $M_t = M_{e1} \{1 - \exp(-k_1 t)\} + M_{e2} \{1 - \exp(-k_2 t)\}$, showing that two independent barriers exist in the *n*-propanol sorption. Therefore, amphiphilic *n*-propanol was sorbed into both hydrophilic and hydrophobic channels. Compound **4b** sorbed hydrophobic dichloromethane, while the amounts for **2b** and **3b** were comparable to or smaller than those of surface adsorption (< 5 μL g^{-1}) (Figure 3C). This is probably because the opening of the hydrophobic channel of 4b (4.0 × 5.2 Å) was large enough to accommodate dichloromethane (d = 4.2 Å), while the opening of the hydrophobic channels of **2b** (2.5 × 5.1 Å) and **3b** (3.4 × 5.1 Å) were too small. The amount of dichloromethane sorption for **4b** around saturation pressure at 273 K was 25 μL g^{-1}. The value fairly agreed with the volume of the hydrophobic channel of **4b** (30.0 ± 3.0 μL g^{-1}), which is in accord with the idea that hydrophobic halocarbons are sorbed only in the hydrophobic channel.

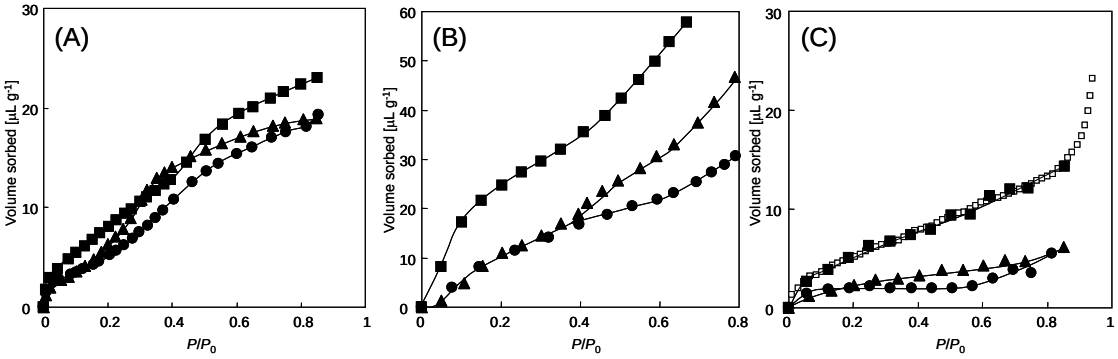

Figure 3. Vapor sorption isotherms of **2b**-**4b** at 298 K. (A) Water, (B) *n*-propanol, and (C) dichloromethane. Circle: **2b**, triangle: **3b**, and square: **4b**. Open squares in (C) showed the results at 273

When **4b** was exposed to a gas flow containing water (P/P_0 = 0.60) and dichloromethane (P/P_0 = 0.40), the weight increased as shown in Figure 4. The best fits for the experimental data by the summation of the linear driving force model were given by $k_1 = 1.7 \times 10^{-2}$ s^{-1}, M_{e1} =16.4 μL g^{-1} (1.64wt%),

$k_2 = 3.0 \times 10^{-3}$ s^{-1}, and $M_{e2} = 7.0$ μL g^{-1} (0.93wt%). The k_1 and M_{e1} values were close to those of water sorption at $P/P_0 = 0.60$ and the k_2 and M_{e2} values were close to those of dichloromethane sorption at $P/P_0 = 0.40$. Therefore, the rate and equilibrium amount of the dichloromethane sorption into the hydrophobic channel and those of water into the hydrophilic channel of **4b** were independent of each other, and the phenomenon was different from those of zeolites and activated carbons, of which the amounts of dichloromethane sorption are decreased by the presence of water.

The collection of dichloromethane and water from the gas mixture was attempted with **4b** according to Scheme 1. Compound **4b** was exposed to the gas mixture of water and dichloromethane at 298 K for 12 h to form **4b**•5.4±0.2H_2O•0.8±0.05CH_2Cl_2. After the removal of the coexisting gases at 203 K, the sample was heated at 273 K and kept for 1.5 h. The amount of dichloromethane evolved was 9.9±0.5 μL g^{-1} (0.70±0.05CH_2Cl_2 per **4b**). Then the sample was evacuated at 298 K for 1.5 h and the amount of water collected was 22±1 μL g^{-1} (5.2±0.2H_2O per **4b**). Thus, dichloromethane and water sorbed in **4b** were successfully collected.

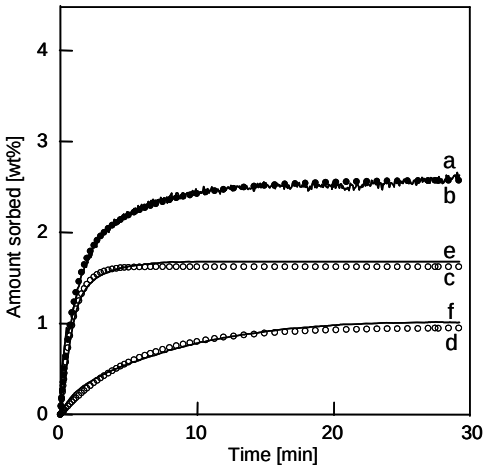

Figure 4. Changes in the weight of **4b** by the exposure to a gas mixture of water and dichloromethane at 298 K. Solid line (a) showed the experimental data. Solid lines (e) and (f) showed the experimental sorption data of water and dichloromethane, respectively. Solid circle (b) showed the calculated data and open circles (c) and (d) showed the two components for the calculation.

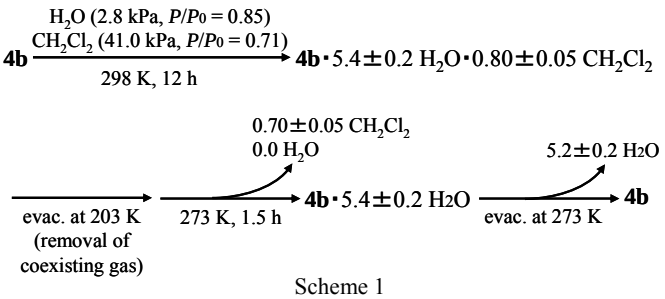

Scheme 1

2. 3D-arrangements of $[M_3O(OOCC_6H_5)_6(H_2O)_3]_4[\alpha\text{-}SiW_{12}O_{40}]$ (M = Cr, Fe) utilizing the π-π stacking

The complexation of $[\alpha\text{-}SiW_{12}O_{40}]^{4-}$ with $[M_3O(OOCC_6H_5)_6(H_2O)_3]^+$ (M = Cr, Fe) was attempted for the aim to utilize the π-π stacking in the arrangement of the macroions and to increase the hydrophobicity of the ionic crystals. Ionic crystals of $[M_3O(OOCC_6H_5)_6(H_2O)_3]_4[\alpha\text{-}SiW_{12}O_{40}]\cdot nH_2O\cdot mCH_3COCH_3$ (M = Cr [**6a**], Fe [**7a**]) were formed from an acetone/water solution. Single crystal X-ray analyses showed that **6a** and **7a** were isostructural. As shown in Figure 1, the macrocations formed 8-membered rings, which incorporated polyoxometalates. The distances between the benzene groups of the neighboring macrocations were 3.4-3.6 Å, and the π-π

interaction probably stabilizes the crystal structure. Compounds **6a** and **7a** sorbed small organic molecules in the crystal lattice and heterogeneously catalyzed the pinacol rearrangement.

3. Monodispersed crystalline nano-particles of $[Ni(tacn)_2]_2[\alpha\text{-}SiW_{12}O_{40}]$

The complexation of $[\alpha\text{-}SiW_{12}O_{40}]^{4-}$ with $[Ni(tacn)]^{2+}$ (tacn = triazacyclononane) yielded monodispersed crystalline nano-particles of $[Ni(tacn)_2]_2[\alpha\text{-}SiW_{12}O_{40}]\cdot 4H_2O$ [**8a**] (Figure 1). The powder X-ray analysis of **8a** showed that the macroions were closely packed into a trigonal cell. The BET surface area of anhydrous form **8b** was 31 $m^2\ g^{-1}$, and the α_s-plot showed that **8b** was non-porous. The average diameter of **8b** calculated with the surface area and density was 51 nm and the value fairly agreed with that of the averaged particle size observed by SEM (59 nm). The formation of nano-particles was probably due to the strong ionic interaction between the multiple-charged macroions ($[\alpha\text{-}SiW_{12}O_{40}]^{4-}$ with $[Ni(tacn)]^{2+}$) and the hydrophobicity of the organic moiety which facilitated the nucleation and prevented the aggregation of the particles. The vapor sorption isotherms showed that **8b** adsorbed hydrophobic tetrachloromethane as well as water and dinitrogen. The complexation of $[\gamma\text{-}SiV_2W_{10}O_{38}(OH)_2]^{4-}$ with $[Ni(tacn)]^{2+}$ yielded crystalline nano-particles of $[Ni(tacn)_2]_2[\gamma\text{-}SiV_2W_{10}O_{38}(OH)_2]\cdot 3H_2O$ [**9a**], which was isostructural with **8a**. Compound **9a** heterogeneously catalyzed the epoxidation of olefins with H_2O_2 maintaining the stereoselectivity of the tetra-*n*-butylammonium salt of $[\gamma\text{-}SiV_2W_{10}O_{38}(OH)_2]^{4-}$ in the homogeneous reaction system.